Extraction of Field Boundaries and Wind Erosion Obstacles from Aerial Imagery[1]

MATTHIAS BUTENUTH[2]

Abstract: In this paper work on image analysis methods extracting field boundaries and wind erosion obstacles from aerial imagery is presented. Describing the objects of interest and additional GIS-data together in an integrated semantic model is essential to get an overview of the numerous relations between the different objects and how to exploit the prior knowledge. The field boundaries and wind erosion obstacles are first extracted separately: A segmentation within selected regions of interest in the imagery leads to field areas, which are split, if necessary, to preliminary fields. Furthermore, a snake algorithm is initialized to correct the geometric inaccuracies in some parts yielding final field boundaries. Wind erosion obstacles are derived using DSM-data in addition to the imagery to verify search areas from the prior GIS knowledge, for example parallel and nearby roads, or to extract wind erosion obstacles without prior information about their location. Finally, a combined evaluation of the different objects is accomplished to exploit the modelled geometrical similarities resulting in a refined and integrated solution.

1   Introduction and Motivation

In this paper work on image analysis methods extracting field boundaries and wind erosion obstacles from aerial imagery is described. This data is needed for various applications, such as the derivation of potential wind erosion risk fields for geo-scientific questions, which can be generated with additional input information about the prevailing wind direction and soil parameters, as described in (THIERMANN ET AL. 2002). Another area is the agricultural sector, where information about field geometry is important for tasks concerning precision farming or the monitoring of subsidies (ANDERSON ET AL. 1999).

In the past, several investigations have been carried out regarding the automatic extraction of man-made objects such as buildings or roads, see for example (MAYER 1998). Similarly, investigations regarding the extraction of trees have been accomplished, see (HILL & LECKIE 1999) for an overview of approaches suitable for woodland and (STRAUB 2003) for a method to extract trees not only capable for woodland but also in the open landscape. It has to be investigated, to what extent these approaches are usable for extracting wind erosion obstacles such as hedges or tree rows, and also which enhancements are necessary to realize the proposed strategy here. In contrary, research with respect to the extraction of field boundaries from high resolution imagery is still not in an advanced phase: (LÖCHERBACH 1998) presented an approach to update and refine topologically correct field boundaries by a fusion of raster-images and vector-map data. Focusing on the reconstruction of the geometry and features of the land-use units, the acquisition of new field boundaries is not discussed. In (TORRE & RADEVA 2000) a so called region competition approach is described, which extracts field boundaries from aerial images with a combination of region growing techniques and snakes. To initialize the process, seed regions have to be defined manually, which is a time and cost-intensive procedure. In (APLIN & ATKINSON 2004) a technique for predicting missing field boundaries from satellite images is presented, using a comparison of modal land

---

cover and local variance. The approach involves manual post processing, because only fields with a high likelihood of missing boundaries are identified, not field boundaries directly. The aim of the solution, presented in this paper, is a fully automatic extraction of field boundaries from high resolution aerial CIR-imagery. Consequently, the proposed strategy differs from the mentioned approaches. In addition, relationships between the objects of interest – field boundaries and wind erosion obstacles – will be exploited to improve the results.

In general, the recognition of objects with the help of image analysis methods starts frequently with a modelling of the objects of interest and the surrounding scene. Furthermore, exploiting the context relations between different objects leads to a more overall and holistic description, see for example (BUTENUTH ET AL. 2003). The use of prior knowledge (e.g. GIS-data) supporting object extraction can lead to better results as shown in (BALTSAVIAS 2004). These aspects are incorporated modelling the extraction of field boundaries and wind erosion obstacles and are reflected in the derived integrated strategy. Initially, the integration of vector and raster data in one semantic model is briefly described in the next section to obtain an overview of the numerous relations between the objects to be extracted and the prior knowledge. Afterwards, the strategy and approach to extract field boundaries and wind erosion obstacles is explained, followed by results to demonstrate the potential of the proposed solution. Finally, further work required is discussed in the conclusions.

2 Semantic Model for the Integration of GIS-data and Aerial Imagery

Describing the integration of GIS-data with aerial imagery in one semantic model is the starting point for object extraction (BUTENUTH 2004). The semantic model is differentiated in an object layer, consisting of the real world, a GIS-layer, a geometric and material part, as well as an image layer (cf. Figure 1). The model is based on the assumption, that the used CIR-images are generated in summer, when the vegetation is in an advanced period of growth. The use of prior knowledge plays an important role, which is represented in the semantic model with an additional GIS-layer. Vector data of the ATKIS DLMBasis (German Authoritative Topographic-Cartographic Information System) is used: (1) Field boundaries and wind erosion obstacles are exclusively located in the open landscape, thus, further investigations are focused to this area. The open landscape is not directly modelled in the ATKIS DLMBasis, this is why this information has to be derived by selecting all areas, which are not settlements, forests or water bodies. (2) The road network, rivers and railways can be used within the open landscape as prior knowledge: The geometries of the GIS-objects are introduced in the semantic model with a direct relation from the GIS-layer to the real world (cf. Figure 1). For example, the ATKIS objects 3101 (road) and 3102 (path) are linked to the road segment of the real world and, thus, are usable as field boundaries (e.g. a road is a field boundary). The modelling of the GIS-objects in the geometry and material layer together with the image layer is not of interest, because they do not have to be extracted from the imagery (depicted with dashed lines in Figure 1). (3) Tree rows and hedges are only captured in the ATKIS-data, if they are longer than 200 m and lie along roads or are formative for the landscape. Therefore, the relation from the GIS-layer to the real world is limited and a modelling in the image layer is also required.

The first object to be extracted, the *field*, is divided in the semantic model in *field area* and *field boundary* in order to allow for different modelling in the layers: The field area is a 2D vegetation region, which is a homogeneous region with a high NDVI (Normalized Difference
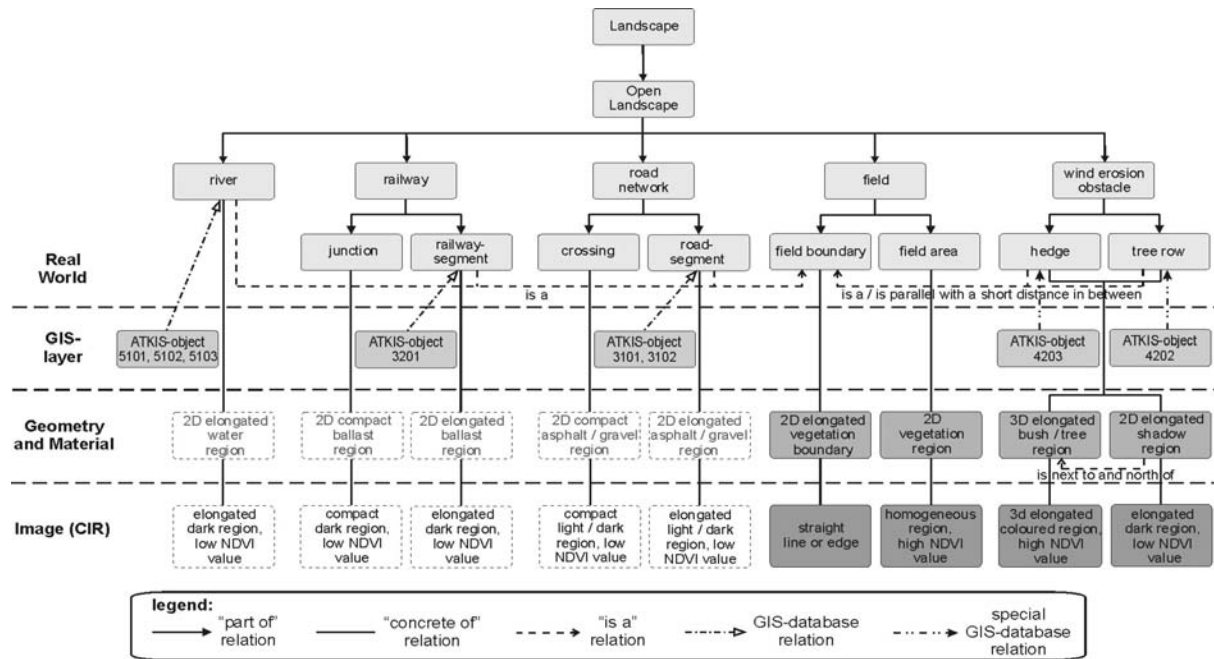
Fig. 1: Semantic Model

Vegetation Index) value in the CIR-image. The field boundary is a 2D elongated vegetation boundary, which is formed as a straight line or edge in the image. Both descriptions lead to the desired result from different sides. The second object to be extracted, the *wind erosion obstacle*, is divided in *hedge* and *tree row* due to different available information from the GIS-layer. Afterwards, both objects are merged, because modelling in the subsequent layers is identical. In addition, the wind erosion obstacles are not only described by their direct appearance in geometry and material, but also with the fact, that due to their height (3D object) there is a 2D elongated shadow region next to and in a known direction (e.g. northern direction at noon). Therefore, the "concrete of" relation not only consists of an elongated, coloured region with a high NDVI value, but additionally of an elongated dark region with a low NDVI value alongside the real object of interest in a known direction. The integrated modelling leads in particular to relationships between the field boundaries and wind erosion obstacles, thus, inside the layers of the semantic model (cf. Figure 1): One object can be part of another one or be parallel and nearby, and together they form a network in the real world. For example, wind erosion obstacles are not located in the middle of a field, because of disadvantageous cultivation conditions, but solely on the field boundaries. Accordingly, the geometries of these different objects are identical or at least parallel with a short distance in between in the case of location alongside roads, rivers or railways.

3 Strategy to Extract Field Boundaries and Wind Erosion Obstacles

3.1 General Strategy

The general strategy for the extraction of field boundaries and wind erosion obstacles is derived from the modelled characteristics of the objects taking into account the realization of an automatic process flow. CIR-images, GIS-data and a Digital Surface Model (DSM) are the input data to initialize the flowchart: Firstly, field boundaries and wind erosion obstacles are

extracted separately with two different algorithms. At a later date, a combined evaluation of the preliminary results due to the modelled geometrical and thematic similarities of the objects is essential getting a refined and integrated solution.

The strategy extracting the *field boundaries* separately starts with the derivation of the open landscape from the GIS-data. In addition, within the open landscape, regions of interest are selected using the road network, rivers, railways, tree rows and hedges as borderlines in order to handle the large datasets in an appropriate manner (cf. Figure 3 for an example of a selected region of interest). Consequently, the borderlines of the regions of interest are field boundaries, which are already fixed, and the image analysis methods are focused to the field boundaries within the regions of interest. The homogeneity of the vegetation of each field enables a segmentation of field areas, processed in a coarse scale to ignore small disturbing structures. Identical vegetation of neighbouring fields leads to missing field boundaries, which can be derived by a line extraction in a finer scale. Further knowledge will be introduced at this time to exploit GIS-data, which gives evidence of field boundaries within the selected regions of interest. The derived field boundaries are in some parts inaccurate and a snake algorithm is initialized to refine their geometric accuracy. The strategy extracting the *wind erosion obstacles* separately starts with a differentiated exploitation of the GIS-data. Focussing on the open landscape, search buffers are defined using the prior knowledge from the GIS-data: Search areas for potential wind erosion obstacles are located alongside roads, rivers or railways as described in the semantic model (cf. section 2) and have to be verified using imagery and DSM-data. In contrary, there is no prior information about the location of all other wind erosion obstacles available. In addition to the extraction of high NDVI-values and higher DSM-values than the surrounding area, characteristics of the wind erosion obstacles as straightness, a minimum length, width and height have to be considered. The aim of the combined evaluation of the preliminary results is to detect discrepancies between field boundaries and wind erosion obstacles due to their modelled geometrical and thematic similarities. For example, it has to be solved, how far the extracted geometric position of two different objects has to be matched, if they are located nearby each other. Similarly, extracted wind erosion obstacles without a corresponding extracted field boundary have to be checked, whether there is a field boundary, too, or whether the extraction of the wind erosion obstacle was wrong. Consequently, the combined evaluation and refined extraction process leads to a consistent and integrative final result.

3.2 Extraction of Field Boundaries

3.2.1 Segmentation of Potential Field Areas

The extraction of field boundaries begins with a segmentation in each region of interest to exploit the modelled similar characteristics and homogeneity of each field. As data source the red channel of the CIR-images is used, which according to our experience fulfils the homogeneity criterion best. To utilize the changing vegetation from one field to the next, the absolute values of the gradient are computed. The topography of the grey values is used to accomplish a watershed segmentation (SOILLE 1999). The resulting basins are marked with their corresponding mean grey value in the red channel. Potential field areas are derived grouping basins, if they lie next to each other and have a low grey value difference, additionally considering a minimum size (cf. Figure 4).

3.2.2 Deriving Missing Field Boundaries by Line Extraction and Grouping

The field areas obtained from the segmentation step are only intermediate results. The reason is, that the case of identical vegetation in neighbouring fields – and therefore a missing boundary – is not taken into account. Accordingly, a line extraction (STEGER 1998) is carried out within each field area to derive missing boundaries. The extracted short pieces of lines are grouped to straight long lines in consideration of a minimum length due to the characteristics of the field boundaries. In addition, intersection points of the lines are calculated, if the end points of the corresponding lines have a minimum distance in between. Furthermore, the lines are extended to the boundaries of the field areas, if the distance lies again below a threshold. Results of the extracted lines are depicted in Figure 4 in white. Further GIS knowledge referring to fixed field boundaries *within* the regions of interest (e.g. dead-end streets or tree rows) is introduced to support the extraction of field boundaries (cf. Figure 4). The field areas are split by the extracted or additionally introduced lines yielding the preliminary field boundaries (cf. Figure 5).

3.2.3 Using Snakes to Improve the Geometric Quality of the Results

The field boundaries are in some part geometrically inaccurate, which is why a classical snake algorithm is used to perform the precise delineation. To initialize the processing, the preliminary field boundaries are taken. Additionally, most fields are four cornered polygons and this knowledge can be exploited by using the information about the four corners as well as the straight boundaries at the sides. Snakes were originally introduced in (KASS ET AL. 1988) as a mid-level algorithm which combines geometric and/or topologic constraints with the extraction of low-level features from images. The principal idea is to define a contour with the help of mechanical properties such as elasticity and rigidity (internal energy) to initialize this contour close to the boundary of the objects. In Figure 2 an example is shown: The preliminary result of the field area is used to initialize the snake (depicted in white) and

Fig. 2: Example for the measurement of the outline with a snake

furthermore the processed different iteration steps are depicted to show the movement of the snake (black lines). The contour can be looked upon as a virtual rubber cord which can be used to detect valleys in a hilly landscape with the help of gravity. If the snake is initialized close enough to the valleys of the landscape, the gravity drags it into the valleys. The "landscape" may be a surface model, an image, or the edges of an image. The movement originates in a field of gradients, which can be computed on the base of an edge detector's result. The *whole energy* of the snake E_{snake}, to be minimized, is the sum of the internal energy $E_{v(s, t)}$ and the external energy E_{ext}, as defined in (KASS ET AL. 1988). The internal energy is described in the following in detail due to the speciality of the here presented work, given in equation (1):
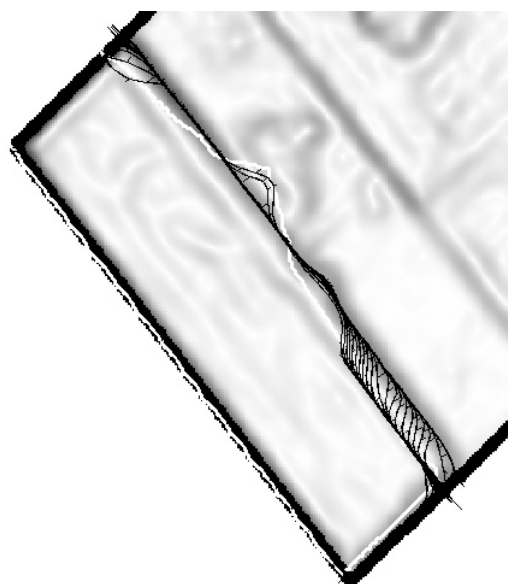
$$E_{v(s,t)} = \tfrac{1}{2}\left(\alpha(s)\cdot\left|v'(s,t)\right|^2 + \beta(s)\cdot\left|v''(s,t)\right|^2\right) \qquad (1)$$

The application *field boundary* leads to a possibility to select special weight functions *α(s) and β(s)*, which are used to control the elasticity and rigidly of the contour *v(s,t)*; *s* is the arc length and *t* the iteration number. The weight functions have to lead to stiff edges along the expected straight lines of the field as well as to allow the snake to form corners. As *external force* the absolute values of the gradients of the given red channel of the imagery are used. Additionally, the boundaries of the region of interest and the further introduced knowledge within the region are manipulated to form "deep valleys" to steer the snake to this fixed boundaries (cf. section 2).

3.3 Extraction of Wind Erosion Obstacles

The strategy extracting wind erosion obstacles is divided into two parts, as described in section 3.1: The definition of buffers alongside GIS-objects as roads, rivers or railways allows a focussed view to narrow search areas. If high NDVI-values can be extracted within the search area, evidence of dense vegetation is given. The additional extraction of higher DSM-values than the surrounding area verifies the potential wind erosion obstacles. Objects not located alongside GIS-objects, have to be extracted without prior information about their location: In a course scale of the NDVI-image, a line extraction of high values is carried out as well as a line extraction of higher DSM-values than the surrounding area. In addition, the geometric model of the wind erosion obstacle has to be introduced processing the extracted short pieces to final objects in consideration of a minimum length, width and height. Another possibility to extract wind erosion obstacles is the use of texture. In addition, the extraction of single trees in a finer scale is an alternative, as for example presented in (STRAUB 2003), and a subsequent linking of the resulting objects to lines, if they are side by side.

4   Results

In this section example results are presented. In Figure 3 the red channel of the imagery of a selected region of interest is depicted, the boundaries of the regions have been derived from the ATKIS-data. The preliminary results of the segmentation are shown in Figure 4, each grey value is one segmented field area. The field areas are superimposed with extracted lines in white and additional further knowledge from the GIS-data in black. The final result of the segmentation step is depicted in Figure 5. It must be recognized, that the geometric correctness is not always satisfying: For example, the field boundaries in the middle top of the depicted region of interest in Figure 5 are not exactly identical to the real boundaries of the field in the image. The initialized snake algorithm is a reasonable possibility to refine these preliminary results, details for one field and the associated iteration steps of the snake algorithm are highlighted in Figure 2. The refined result of the extraction of field boundaries is depicted in Figure 6. The geometric correctness has improved, but the topological correctness has in some parts suffered. The realization of the proposed strategy extracting wind erosion obstacles is still in progress, which is why results in this domain are not depicted.

5   Conclusions

In this paper work on the automatic extraction of field boundaries and wind erosion obstacles from aerial imagery is presented. A semantic model integrating the different objects to be extracted and the GIS-data is described. Next, the derived strategy is discussed considering

Fig.3: Selected region of interest, depicted is the red channel of the aerial image
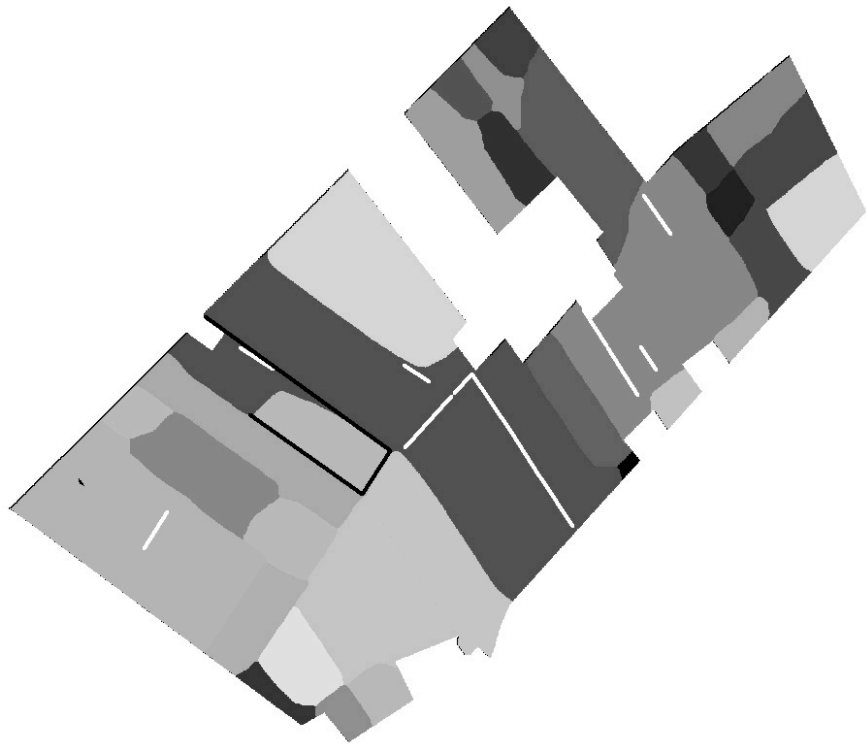

Fig. 4: Preliminary segmentation result, additionally superimposed with extracted lines (white) and further knowledge (black)
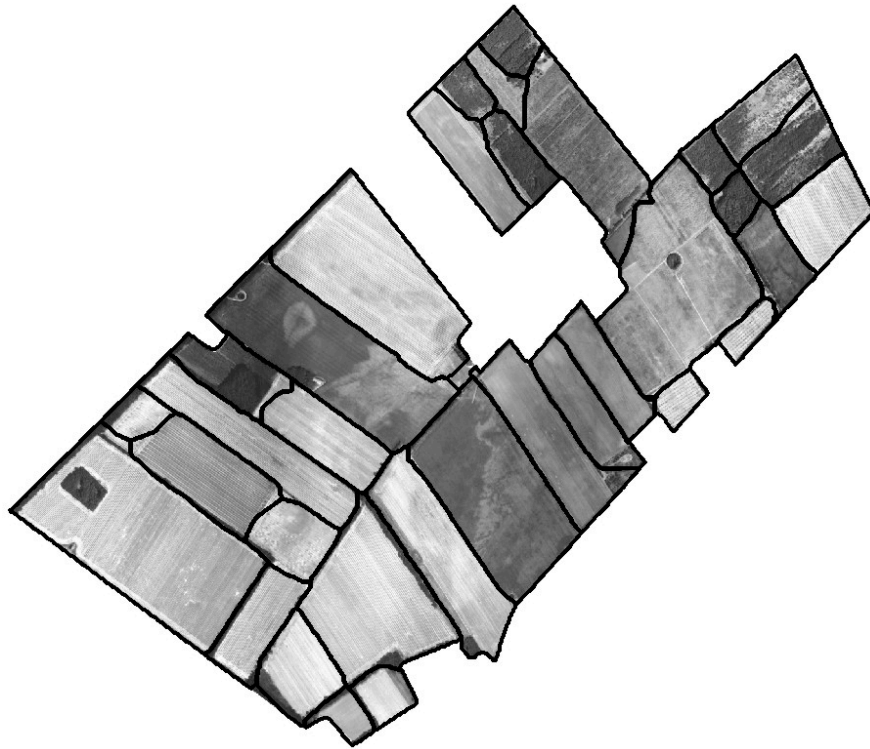
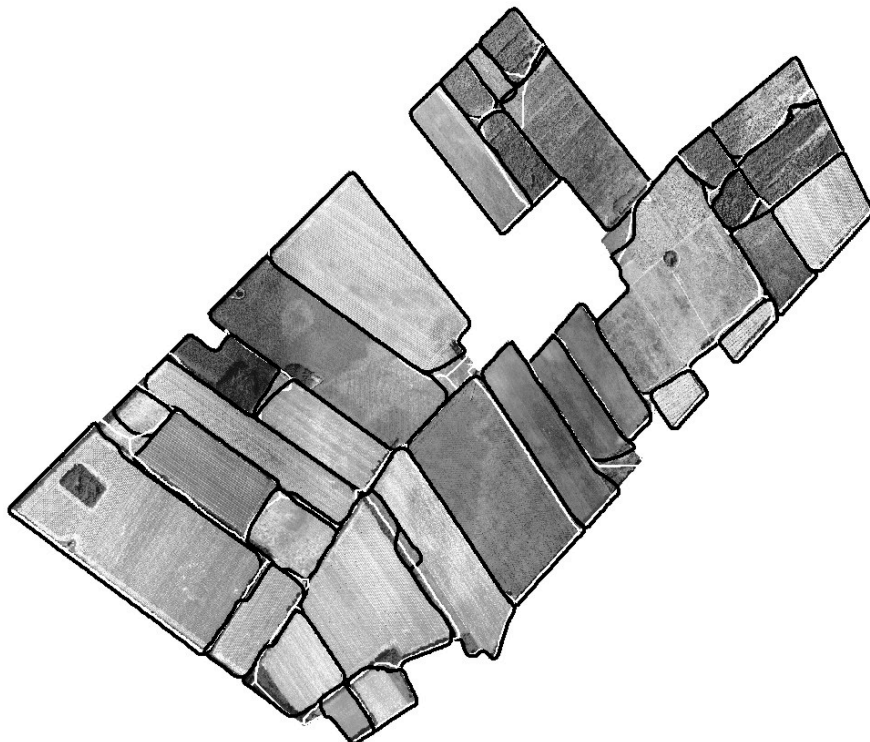Fig. 5: Result of the preliminary field boundaries is depicted in black

Fig. 6: Refined result of the field boundaries after the snake-processing: Initialization is depicted in white, field boundaries are depicted in black

an automatic processing flow: The strategy is divided to extract the objects of interest separately. The segmentation of field areas based on the gradients in coarse scale of the imagery is carried out using a watershed segmentation. In the future, the use of colour and/or texture may stabilize the segmentation step. Extracted and grouped lines with different criteria in a fine scale and additional introduced prior knowledge from GIS-data divide the field areas in detailed and improved preliminary results. Finally, the derived field boundaries are geometrically refined using a snake algorithm. The results demonstrate the potential of the proposed solution. Future work will be devoted to the development of an integrated network of snakes for all field areas of the region of interest together, not only a snake initialization for each field separately, in order to improve the topological correctness. The proposed strategy concerning the extraction of wind erosion obstacles has to be investigated in detail and the derived results have to be evaluated. In addition, future work will be done on the combined evaluation of the different objects deriving a refined and integrated final result.

Acknowledgements

References

ANDERSON, J. E., FISCHER, R. L. & DELOACH, S. R., 1999: Remote Sensing and Precision Agriculture: Ready for Harvest or Still Maturing? Photogrammetric Engineering & Remote Sensing, Vol. 65, No. 10, pp. 1118-1123.

APLIN, P. & ATKINSON, P. M., 2004: Predicting Missing Field Boundaries to Increase Per-Field Classification Accuracy. Photogrammetric Engineering & Remote Sensing, Vol. 70, No. 1, pp. 141-149.

BALTSAVIAS, E. P., 2004: Object Extraction and Revision by Image Analysis Using Existing Geodata and Knowledge: Current Status and Steps towards Operational Systems. ISPRS Journal of Photogrammetry and Remote Sensing, Vol. 58, No. 3-4, pp. 129-151.

BUTENUTH, M., 2004: Modelling the Extraction of Field Boundaries and Wind Erosion Obstacles from Aerial Imagery, International Archives of the Photogrammetry, Remote Sensing and Spatial Information Sciences, Istanbul (to appear).

BUTENUTH, M., STRAUB, B. M., HEIPKE, C. & WILLRICH, F., 2003: Tree Supported Road Extraction from Aerial Images Using Global and Local Context Knowledge, In: Crowley Piater Vincze Paletta (Eds.), Lecture Notes in Computer Science, Springer Verlag, Graz, Austria, Vol. LNCS 2626, pp. 162-171.

HILL, D. A. & LECKIE, D. G. (Eds.), 1999: International forum: Automated interpretation of high spatial resolution digital imagery for forestry, February 10-12, 1998, Natural Resources Canada, Canadian Forest Service, Pacific Forestry Centre, Victoria, British Columbia, 395 p.

KASS, M., WITKIN, A. & TERZOPOULUS, D., 1988: Snakes: Active Contour Models. International Journal of Computer Vision, Vol. 1, pp. 321-331.

LÖCHERBACH, T., 1998: Fusing Raster- and Vector-Data with Applications to Land-Use Mapping, Inaugural-Dissertation der Hohen Landwirtschaftlichen Fakultät der Universität Bonn, Bonn, 107 p.

MAYER, H., 1998: Automatische Objektextraktion aus digitalen Luftbildern, Habilitation Reihe C, Deutsche Geodätische Kommission, München, No. 494.

SOILLE, P. (Ed.), 1999: Morphological Image Analysis: Principles and Applications, Springer, Berlin Heidelberg New York, 316 p.

STEGER, C., 1998: An unbiased detector of curvilinear structures, In: IEEE Transactions on Pattern Analysis and Machine Intelligence (Eds.), Vol. 20, No. 2, pp. 311-326.

STRAUB, B. M., 2003: Automatische Extraktion von Bäumen aus Fernerkundungsdaten, Dissertation Reihe C, Deutsche Geodätische Kommission, München, No. 572, 99 p.

THIERMANN, A., SBRESNY, J. & SCHÄFER, W., 2002: GIS in WEELS - Wind Erosion on Light Soils. GeoInformatics, No. 5, pp. 30-33.

TORRE, M. & RADEVA, P., 2000: Agricultural Field Extraction from Aerial Images Using a Region Competition Algorithm, International Archives of Photogrammetry and Remote Sensing, Amsterdam, Vol. XXXIII, No. B2, pp. 889-896.